Journal of
Materials Chemistry C

ROYAL SOCIETY
OF **CHEMISTRY**

COMMUNICATION

Check for updates

Cite this: *J. Mater. Chem. C*, 2024, **12**, 19352

Received 17th September 2024,
Accepted 12th November 2024

DOI: 10.1039/d4tc03970j

rsc.li/materials-c

Heterometallic NIR-emitting nanothermometers by click-reaction between two lanthanide complexes†

Daniil. S. Koshelev,*[ab] Aleksei V. Medved'ko,[c] Alexander S. Goloveshkin,[d] Yulia V. Nelubina,[d] Olga A. Maloshitskaya,[b] Elnara S. Safiullina,[df] Yulia A. Gracheva,[b] Evgeny A. Nikitin,[b] Leonid S. Lepnev,[e] Sergey Z. Vatsadze[c] and Valentina V. Utochnikova*[ab]

Heterobimetallic lanthanide conjugates were obtained by click-reaction between two monometallic lanthanide complexes with Schiff bases for the first time. For that, novel azido- and ethynyl-substituted ligands, as well as their lanthanide complexes, were obtained and characterised; two new crystal structures were obtained. Click-reaction between ligands and complexes was performed, and the latter was demonstrated to result in the conjugates {Ln_1–Ln_2} formation. Among the obtained conjugates, {Yb–Nd} and {Yb–Er} demonstrated intense NIR emission with temperature sensitivity in the physiological range of up to 3%/K.

Heterobimetallic lanthanide compounds demonstrate a wide field of potential applications, particularly in areas such as sensors,[1,2] thermometry,[3–5] up-conversion,[6–8] tomography[9,10] and imaging.[11–13] Due to the high lability of lanthanide compounds and similar lanthanide ions radii,[14] it is challenging to produce heterobimetallic compounds in the form of isolated molecules, due to metal ions exchange. This could be provided by obtaining helicates[8,13,15,16] but not for close pairs such as Tb/Eu or Er/Yb. A promising approach is to directly combine two monomeric luminescent lanthanide complexes to form a bimetallic conjugate.[17,18] However, due to the lability of the lanthanide complexes, it is required very strongly linked compounds like DOTA-species[17–20] as precursors for the reaction. The resulting DOTA-containing complexes demonstrate moderate luminescent properties. As alternative precursors for near-infrared (NIR) luminescent heterobimetallic conjugates, we promote monometallic lanthanide complexes with substituted Schiff bases ((derivatives of *N*-(2-((2-benzoyl) hydrazineylidene)methyl)phenyl)-4-methylbenzene-sulfonamide or H_2L), that have demonstrated excellent solubility,[21,22] non-toxicity,[23] luminescence efficiency in the NIR region,[24] and high absorption.[23] As a combination mechanism, we suggest click-reaction, for instance, the copper(I) catalyzed azide–alkyl cycloaddition. In this paper, we proposed to use this click-reaction of monometallic mononuclear lanthanide complexes with Schiff bases to obtain heterobimetallic compounds of a given composition for lanthanide ions. This task has been broken down into several sequential steps: first, to obtain dissociation-resistant complexes with azidomethyl- and ethyl-substituted Schiff bases. Second, to conduct the click-reaction between Schiff bases, to confirm the possibility of such a reaction and the absence of interfering factors from the catalyst, for example, the formation of copper complexes with the departure of catalyst ions from the reaction. Third, to prepare lanthanide complexes with a Schiff base obtained as a result of the click-reaction of ligands to prove the complexation ability of the new ligand. Fourth, to implement a click-reaction between homometallic lanthanide complexes with rising difficulty levels from only diamagnetic complexes of lutetium up to heterobimetallic erbium and ytterbium complexes.

Particular attention while analyzing the complex composition was paid to the ^1H NMR spectra data, which is particularly informative for Ln-containing species due to the lanthanide-induced shift (LIS) and broadening,[25–27] and MALDI MS which is very informative due to specific isotopic distribution of lanthanides.[28,29]

The syntheses of the ligands H_2L = H_2L1 and H_2L2 were carried out through condensation of the benzaldehydes and

---

[a] *Faculty of Material Sciences, Lomonosov Moscow State University, 1/73 Leninskie gory, Moscow, 119991, Russia. E-mail: daniil.s.koshelev@gmail.com, valentina.utochnikova@gmail.com*
[b] *Department of Chemistry, Lomonosov Moscow State University, 1/3 Leninskie gory, Moscow, 119991, Russia*
[c] *Zelinsky Institute of Organic Chemistry RAS, 47 Leninsky Prospekt, Moscow, 119991, Russia. E-mail: vatsadze@ioc.ac.ru*
[d] *A. N. Nesmeyanov Institute of Organoelement Compounds, Russian Academy of Sciences, 119334Vavilova St. 28, bld. 1, Moscow, Russia*
[e] *P. N. Lebedev Physical Institute of the Russian Academy of Sciences, GSP-1, Moscow, Leninsky Prospekt, 53, GSP-1, Moscow, 119991, Russia*
[f] *A.V. Topchiev Institute of Petrochemical Synthesis, RAS, 29 Leninskiy pr., 119991, Moscow, Russia*

† Electronic supplementary information (ESI) available. CCDC 2364377 and 2367003. For ESI and crystallographic data in CIF or other electronic format see DOI: **https://doi.org/10.1039/d4tc03970j**

4-(azidomethyl)-benzohydrazide or 4-(ethynyl)-benzohydrazide.[30] The 2-(*N*-tosylamino)benzaldehyde was obtained during the procedure described earlier.[31] The 4-(azidomethyl)-benzohydrazide was obtained by a 3-step procedure described earlier.[23,32,33] The 4-(ethynyl)-benzohydrazide was obtained by a 3-step procedure described earlier.[34,35] After each step, the purity of the products was monitored by ^{1}H NMR spectroscopy (Fig. S4–S6 and S9–S11, ESI†).

Synthesis of Ln(L)(HL) (Ln = Yb, Lu; L = L1 or L2) was performed by the reaction between the freshly prepared $Ln(OH)_3$ and the ligand H_2L in ethanol:acetonitrile (EtOH : ACN = 1 : 1).[36]

Synthesis of $K[Ln(L)_2](H_2O)_n$ (Ln = Nd, Gd, Er, Yb, Lu; L = L1 or L2) were obtained during the reaction between Ln(L)(HL) in the ethanol : THF (1 : 1) mixture with the stoichiometric amount of pre titrated KOH solution in EtOH (see ESI† – synthesis of lanthanide complexes):

$$Ln(L)(HL) + KOH \rightarrow K[Ln(L)_2](H_2O)_n \quad (n = 2 \text{ for L1; 1 for L2})$$

The obtained complexes were analyzed using PXRD and TGA data (Fig. S15–S17, ESI†), as well as MALDI-TOF mass-spectra, demonstrating the presence of the corresponding *m*/*z* of the complexes with the characteristic isotopic distribution of corresponding lanthanides (Yb, Er, Nd) (Fig. S18, ESI†).

Single crystals were obtained for Er(L2)(HL2), $K[Nd(L1)_2]$(THF), by THF/*n*-hexane diffusion mixing with subsequent crystallization. The structure of Er(L2)(HL2) consists of two symmetry-independent monomeric species [Ln(**L**)(H**L**)] (Fig. 1). Complexes $K[Nd(L1)_2]$(THF) and $K[Yb(L2)_2]$(THF) demonstrate polymeric structures, in which the mononuclear fragment of $[Ln(\mathbf{L})_2]^-$ links with two potassium ions through the hydrazide fragment and the sulfoxide-fragment.

CuAAC reaction between ligands H_2L1 and H_2L2 was conducted under argon in a methanol solution. The obtained slightly yellow powder of H_4L3 demonstrated low solubility in methanol (<0.5 g L^{-1}) and in THF (<2 g L^{-1}). The product was analyzed by 1D NMR spectroscopy (Fig. S13, ESI†). Lanthanide complexes with H_4L3 anions were obtained similar to those with H_2L1 and H_2L2 anions to ensure the possibility of their formation, as well as to obtain the reference spectra for further click-reaction products analysis (Fig. S15j, k, m, S17i, k, S18j, k and S19, ESI†).

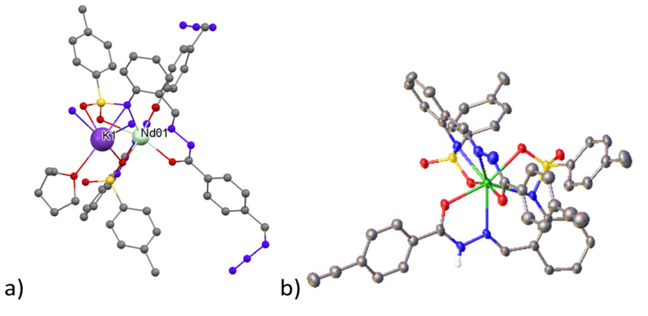

Fig. 1 General view of (a) $K[Nd(L1)_2]\cdot THF$, (b) Er(L2)(HL2) in the representation of atoms *via* thermal ellipsoids at 30% probability level; hydrogen atoms except those of NH groups omitted for clarity.

CuAAC reaction between lanthanide complexes $K[Ln(\mathbf{L})_2](H_2O)_n$ (L = L1, L2, Ln = Nd, Er, Yb, Lu) was studied stepwisely. Initially, to simplify the NMR spectra analysis, two lutetium complexes were subject to CuAAC reaction during one week (Scheme 1), and the precipitated {Lu–Lu} conjugate was analyzed by ^{1}H NMR (Fig. 2) and MALDI-TOF spectra (Fig. 4). MALDI-TOF data is very informative due to specific isotopic distribution and allows us to directly analyze the nuclearity of the detected species. It immediately demonstrates the formation of the {Lu–Lu} conjugate by the presence of the intense signal at 2152 *m*/*z* with the desired distribution.

As each of the complexes has two reactive groups, the product of the reaction can contain both dimers and/or oligomers or even polymers, which is expected to depend on the reaction time. To determine the prevailing product, ^{1}H NMR spectra were analyzed. It was also aimed at the revealing of the most informative ranges which will further help to analyze the NMR data of complexes, containing paramagnetic ions, *i.e.* Yb, Nd, and Er, and even their combinations.

Most of the signals of the initial complexes and the products overlap, which complicates their analysis, unlike the signal of the CH_2-group, which was observed in the 1H spectrum of the H_4L3 at 5.56 ppm. In the spectrum of the {Lu–Lu} conjugate this ligand is also clearly present, proving the course of the reaction. This signal splits into 9 signals with an overall intensity equal to 2H, which corresponds to the average length of the oligomer equal to 8 monomers. To support this conclusion, we also analyzed the signals in the range of 4.2–4.6 ppm, which in spectra of $K[Lu(\mathbf{L})_2](H_2O)$ (**L** = L1, L2) correspond to ethynyl- and azidomethyl groups with intensity 1H and 2H. If {Lu–Lu} dimer is formed, those signals should be presented in the intensity of 2H and 1H, while in the experimental spectrum of {Lu–Lu} there intensity is only 2/8H and 1/8H. This also indicates the oligomeric nature of this conjugate with the average length of the oligomer of 8 monomers.

The FTIR spectra of conjugates are almost identical to the spectra of the initial complexes. However, it is possible to observe the disappearance of the CH-vibration band of the ethynyl fragment due to the formation of triazole. Comparison of conjugate spectra with each other shows their identity (Fig. 3).

Limiting the reaction time down to 24 h to avoid oligomerization, we obtained conjugates {Yb–Lu} and {Yb–Yb} by the same reaction (Scheme 1). Their MALDI MS demonstrated broad isotopic distribution corresponding to the desired mass and desired pair of lanthanides, proving the dinuclear conjugation (Fig. 4). Further analysis was based on the ^{1}H NMR data, which is complicated due to the lanthanide-induced shifts and broadening. At the same time, these difficulties also bear additional information about the compound formed (Fig. 5).

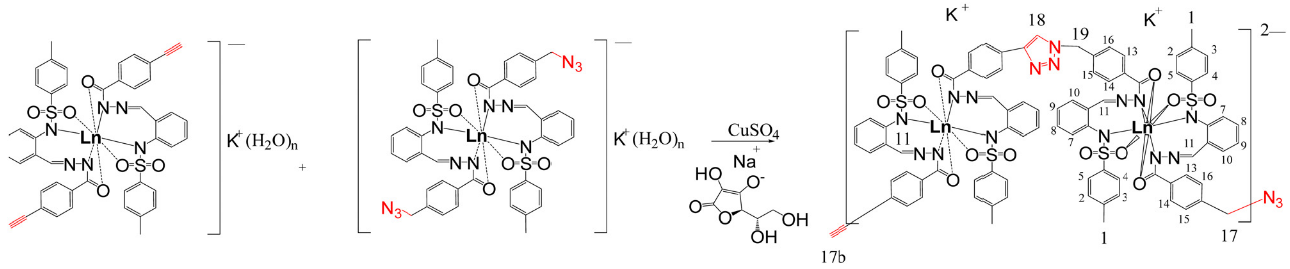

Scheme 1 Synthesis of the {Ln–Ln} conjugates form **K**[Ln(L)$_2$](H$_2$O) (Ln = Nd, Er, Yb, Lu; **L** = L1 or L2).

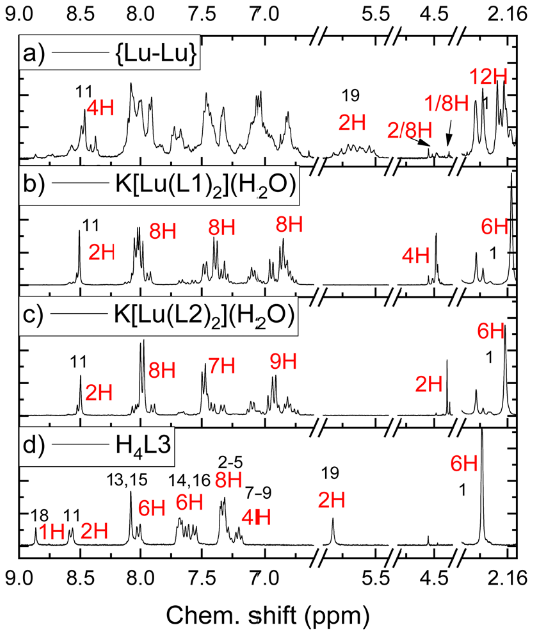

Fig. 2 ^{1}H NMR spectra of (a) {Lu–Lu}, (b) K[Lu(L1)$_2$](H$_2$O), (c) K[Lu(L2)$_2$](H$_2$O), (d) H$_4$L3.

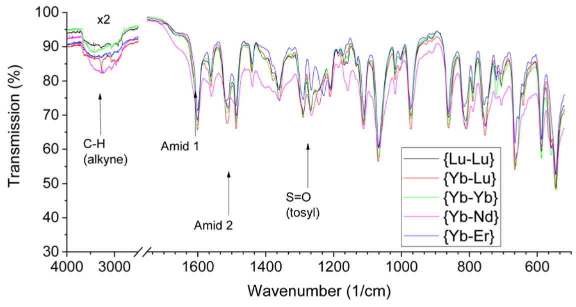

Fig. 3 FT-IR spectra of conjugates.

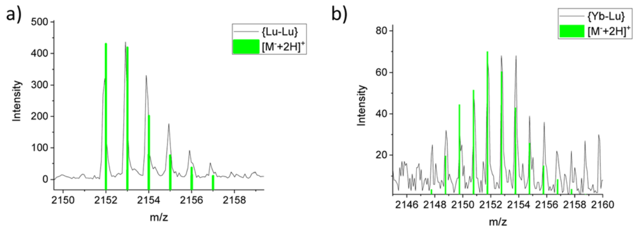

Fig. 4 MALDI-TOF spectra of (a) {Lu–Lu}, (b) {Yb–Lu}.

First of all, we can clearly observe the same signal of the protons (19) in the range of 5.82 ppm and the signals of 17 and 17b protons in the range of 4.2–4.6 ppm, which correspond to ethynyl- and azidomethyl groups with intensity 1H and 2H, proving dinuclearity. These protons are remote from the metal centres which ensures the absence of their shift and therefore facilitates their analysis. Besides, we analyzed the more remote and broadened signals in the spectrum of {Yb–Lu} conjugate, *i.e.* 23.3, 16.4, −13.4, −14.3, −16.8 ppm (see Table S2, ESI†). They were ascribed based on the data published by some of us earlier.[37] We clearly observe those signals with integral intensity equal to $\frac{1}{2}$H; this witnesses the formation of 1 : 1 conjugate. The absence of the exchange between metals – which is the most important question when analysing the product of the click-reaction – is witnessed by the absence of the splitting of these signals. This means that there is only one position of ytterbium ion, while the second position is occupied by Lu ion, and their signals correspond to the protons of the ligand coordinated by lutetium and are not shifted.

It is also worth noting that in the ^{1}H NMR spectrum of the {Yb–Lu} conjugate the signals can be found which broaden to different degrees. We can clearly see the narrow bands of the protons corresponding to the ligand coordinated by lutetium, *i.e.* at the range of 7.0–6.7 ppm corresponding to the proton 7–9. While in the range of 8.6–8.5 or 2.1–1.9, we clearly observe broad bands of the protons within the ligands coordinated by Yb. This also clearly indicates the exact position of each of the metals in the obtained conjugate and the absence of their exchange. Now in the spectrum of the {Yb–Yb} conjugate, the signals at 23.3 to 16.4 ppm and −12 to −15 ppm increase twice in intensity which is in line with the substitution of diamagnetic Lu with paramagnetic Yb. The signals mustn't simply increase in intensity, but additional signals appear in a similar range. This difference in the position, even small, indicates the difference of the ligands coordinated by each of the ions. Such a splitting of the signal present in the spectrum of {Yb–Yb} and absent in the spectrum of {Yb–Lu} proves again that no exchange of

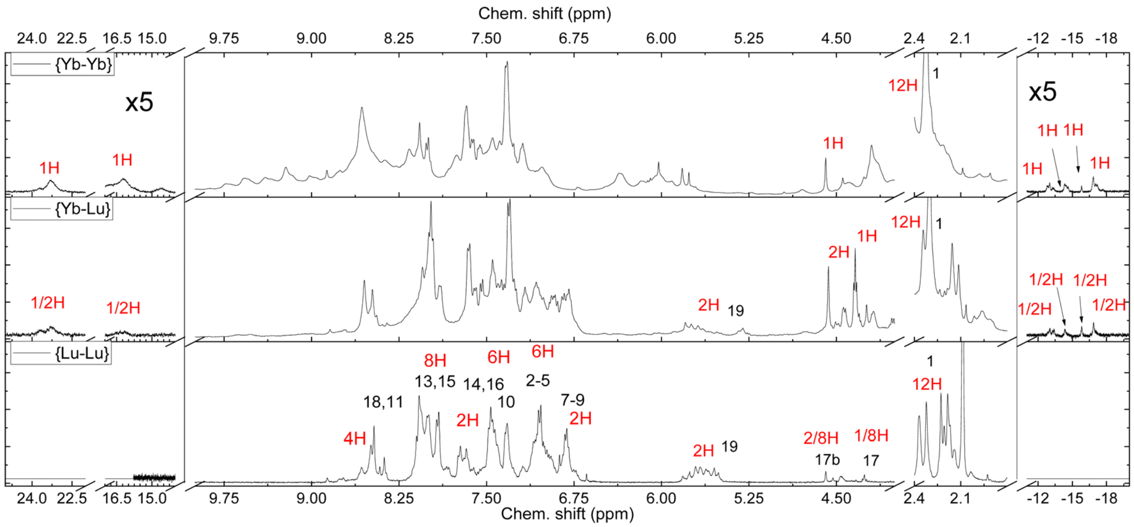

Fig. 5 ^{1}H NMR spectra of {Lu–Lu}, {Yb–Lu}, and {Yb–Yb} conjugates.

metals is observed in the latter case. It is also worth noting that the narrow bands of the protons 7–9 broaden and shift in the spectrum of {Yb–Yb} due to both metals being paramagnetic.

Finally, we conducted the click-reaction to obtain {Yb–Nd} and {Yb–Er} complexes, its product was also analysed by MALDI MS, which demonstrates the signals of the desired species (see Fig. S22, ESI†), and ^{1}H NMR spectroscopy (Fig. S25 and S26, ESI†).

Thermal analysis of the conjugates demonstrate the presence in their composition 3–4 solvate molecules of water or THF due to the corresponding mass losses and ionic currents (m/z = 17, 18 or 72) (Fig. 6).

Most of the conjugates produced were almost amorphous. However, the {Yb–Er} conjugate showed some degree of crystallinity, although it did not exhibit diffraction patterns similar to those of the original complexes.

The latter demonstrates the appearance of the signals at 5.6–6.2 ppm, corresponding to the protons (19), and the appearance of the additional signals, differently broadened and shifted, which correspond to the ligands, coordinated by the second paramagnetic ion (Er in the case of Fig. 7). Here it is very important to mention that the signals of the protons corresponding to the ligand coordinated by Yb ion do not even slightly change their position in conjugates {Yb–Lu}, {Yb–Yb}, {Yb–Nd}, and {Yb–Er}. This indicates the absence of the metal exchange and the appearance of any kind of superposition in every signal, while every signal corresponds to the proton of the certain ligand coordinated by the certain metal.

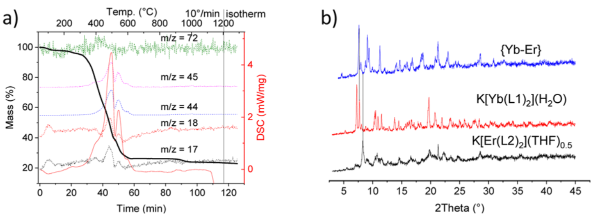

Fig. 6 (a) TGA of {Lu–Lu}, (b) XRD of {Yb–Er} and its precursors.

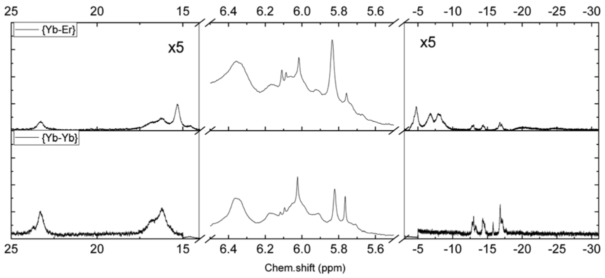

Fig. 7 ^{1}H NMR spectra of {Yb–Er} and {Yb–Yb} conjugates.

Luminescent properties were studied for each of the obtained NIR-emitting complexes (see Table 1). It revealed that the lanthanide complexes possess typical narrowband lanthanide luminescence centred at 980 nm (Yb^{3+}), 860 and 1060 nm (Nd^{3+}), and 1450 nm (Er^{3+}) under 365 nm excitation by UV diode (Fig. S20, ESI†).

For Yb^{3+} complexes, absolute quantum yields and observed lifetimes (τ_{obs}) in the NIR range were measured in powders and DMSO (Table 1), as well as absorption coefficients and ligand triplet states (E_T = 19 230 cm^{-1} for L = L2) were obtained (see Fig. S29–S31, ESI†). Yb(**L**)(H**L**) and K[Yb(**L**)$_2$](H$_2$O)$_n$ demonstrated different QY tendencies.

In case L = L1, K[Yb(**L**)$_2$](H$_2$O)$_n$ possess higher QY, in case of L = L2, Yb(**L**)(H**L**) emitted more efficiently. To understand the reason for that behaviour, we calculated separately the sensitization efficiency (η_{sens}) and an internal quantum yield ($\mathrm{QY}_{\mathrm{Ln}}^{\mathrm{Ln}}$), which are the factors of the external quantum yield ($\mathrm{QY}_{\mathrm{Ln}}^{\mathrm{L}} \equiv$ QY). These data demonstrated that the low sensitization

Table 1 Luminescence characteristics of the obtained complexes and conjugates

	QY^{L}_{Ln}, %		
	Powder	DMSO	τ_{obs}, μs
Yb(L1)(HL1)[23]		1.04 (9)	15.7 (2)
$K[Yb(L1)_2](H_2O)_2$*	1.27	1.5 (13)	22.6 (2)
Yb(L2)(HL2)	1.1	0.85	11.3
$K[Yb(L2)_2](H_2O)$	1.0	0.58	14.0
Nd(L1)(HL1)	0.11	—	1.4
$K[Nd(L1)_2](H_2O)$	0.10	—	1.2
Nd(L2)(HL2)	0.07	—	1.5
$K[Nd(L2)_2](H_2O)$	0.02	—	1.4
$Yb_2(HL3)_2(THF)_{0.5}(H_2O)$	0.67	1.58	10.2
{Yb–Lu}	0.2		11.6
{Yb–Yb}	0.16		8.8
{Yb–Nd}	0.32	0.66	20.7
{Yb–Er}	0.13	0.30	20.8

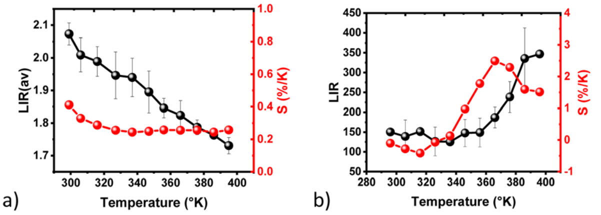

Fig. 8 Luminescent spectra thermometry for powders of (a) {Yb–Nd} (LIR = I980/I1060), (b) {Yb–Er} (LIR = I980/I1460). Excitation 365 nm.

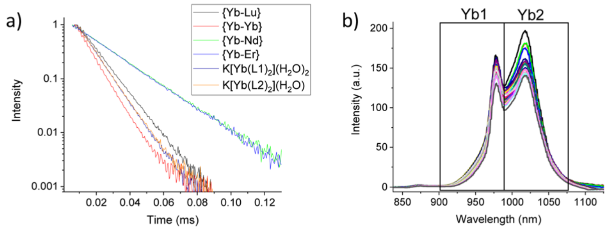

Fig. 9 (a) Monoexponential decay curves of the obtained conjugates (λ_{lum} = 980 nm, λ_{ex} = 337 nm). (b) Temperature dependence of the luminescence spectra of {Yb–Nd}.

efficiency limits the QY value, which could be explained by the huge energy gap between ligand and lanthanide excited states. The obtained complex of Yb^{3+} with H_4L_3 ligand showed both *vis* ligand-centred and NIR metal-centred luminescence with QY up to 1.6% in DMSO solution and absorption up to 60 600 (1/M cm).

The obtained bimetallic conjugates containing luminescent Yb^{3+} ion demonstrated its luminescence, as well as the low intensity, yet detectable luminescence of Nd or Er. Luminescence lifetimes and quantum yields are given in Table 1.

Luminescent decay curves of the obtained conjugates are perfectly monoexponential proving the formation of the individual complexes (Fig. 9). The lifetime values which they demonstrate clearly differ from those of the initial monometallic precursors, witnessing the course of the click-reaction. In comparison with monometallic complexes of NIR-emitting lanthanides, bimetallic conjugates {Yb–Lu} and {Yb–Yb} demonstrate a 5-fold decrease in the photoluminescence quantum yield and an approximately 2-fold decrease in the lifetime of the excited state of ytterbium, which can be attributed to a reduction in the concentration of luminescent ions in the case of Yb–Lu or mutual quenching of two Yb^{3+} cations in the case of {Yb–Yb}. Additionally, the energy transfer between excited states of lanthanide ions confirms an increase in radiative decay time during the sensitized Yb luminescence from excited states of Nd and a decrease in radiative lifetime for the Yb luminescence during sensitized luminescence of Er (Table S1, ESI†). Simultaneously, the observed lifetimes calculated from a monoexponential fit of the relaxation kinetics in the case of {Yb–Lu} and {Yb–Yb} conjugates decreased relative to monometallic compounds, and for {Yb–Nd} and {Yb–Er} conjugates increased, which also indicates energy transfer between lanthanide cations.

The obtained conjugates were tested as luminescent thermometers. For the {Yb–Nd} conjugate, redistribution of energy was observed between the poles of the Stark splitting in the ytterbium luminescence band, and for the {Yb–Er} conjugate, changes in the ratio of ytterbium to erbium luminescence were observed. Luminescence intensity ratio (LIR) parameter was chosen for {Yb–Nd} conjugate intensity ratio between the poles of the Stark splitting in the ytterbium luminescence bands, because the ratio between Nd and Yb luminescence bands demonstrate no correlation with temperature changes.

Relative sensitivity (S_r) was calculated by formula:

$$S_r = 100\% \frac{\mathrm{dLIR}}{\mathrm{LIR} \cdot \mathrm{d}T}$$

Both complexes demonstrated temperature dependence of luminescence in the range 295–395K with sensitivity up to 0.45%/K for {Yb–Nd} and 3%/K for {Yb–Er} conjugates (Fig. 8).

Conclusions

Click-reaction between the lanthanide complexes with non-DOTA-like ligands was conducted for the first time. For that, novel azidomethyl-(H_2L1) and ethynyl-substituted (H_2L2) Schiff bases were obtained, and their lanthanide complexes were synthesized; two new crystal structures were obtained for them. Click-reaction successfully took place, and the heterobimetallic complex formation was proved by MALDI MS and NMR spectroscopy. Heterobimetallic {Yb–Nd} and {Yb–Er} conjugates demonstrated NIR emission of both ions, which was found to be temperature-dependent. The relative sensitivity of the thermometer reached 0.45 and 3%/K respectively.

Author contributions

	Daniil .S. Koshelev	Alexey V. Medved'ko	Alexander.S. Goloveshkin	Yulia V. Nelubina	Olga A. Maloshitskaya	Elnara S. Safiullina	Yulia A. Gracheva	Evgeny A. Nikitin	Leonid S. Lepnev	Sergey Z. Vatsadze	Valentina V. Utochnikova
Conceptualization	Lead	Low									Eq.
Data curation	Lead	Low	Eq.	Low	Low	Low	Low	Low	Low	Low	
Formal analysis	Eq.										Eq.
Funding acquisition	Lead										Eq
Investigation	Lead	Low	Low	Low	Low	Low	Low	Low	Low	Low	
Methodology	Eq.	Eq.									Eq.
Project administration	Eq.										Eq.
Resources	Eq.	Low	Low	Low	Low	Low	Low	Low	Low	Low	Eq.
Software	Eq.										
Supervision											Lead
Validation	Eq.	Low	Low	Low	Low	Low	Low	Low	Low	Low	Lead
Visualization	Eq.		Low	Low							
Writing – original draft	Lead	Low	Low	Low	Low	Low	Low	Low	Low	Low	Eq.
Writing – review & editing	Eq.										Lead

Data availability

The data supporting this article have been included as part of the ESI.† Crystallographic data for K[Nd(L1)$_2$](THF) and Er(L2)(HL2) has been deposited at the CCDC under 2364377 and 2367003.

Conflicts of interest

There are no conflicts to declare.

Acknowledgements

We thank the Russian Science Foundation (grant #23-23-00293) for financial support. The research was carried out under partial not financial support of MSU Shared Research Equipment Center ''Technologies for obtaining new nanostructured materials and their complex study'', National Project ''Science'' and MSU Program of Development. The XRD studies were performed using the equipment of the Center for Molecular Composition Studies of INEOS RAS with the support of the Ministry of Science and Higher Education of the Russian Federation (Contract No. 075-00277-24-00). With great respect, we dedicate this work to Prof. Jean-Claude G. Bünzli on the occasion of his 80th anniversary.

Notes and references

1 H. Zhang, R. Fan, W. Chen, J. Fan, Y. Dong, Y. Song, X. Du, P. Wang and Y. Yang, *Cryst. Growth Des.*, 2016, **16**, 5429–5440.

2 N. Iki, *Supramol. Chem.*, 2011, **23**, 160–168.

3 K. Karachousos-Spiliotakopoulos, V. Tangoulis, N. Panagiotou, A. Tasiopoulos, E. Moreno-Pineda, W. Wernsdorfer, M. Schulze, A. M. P. Botas and L. D. Carlos, *Dalton. Trans.*, 2022, **51**, 8208–8216.

4 V. Tangoulis, V. Nastopoulos, N. Panagiotou, A. Tasiopoulos, G. Itskos, M. Athanasiou, E. Moreno-Pineda, W. Wernsdorfer, M. Schulze and O. Malina, *Inorg. Chem.*, 2022, **61**, 2546–2557.

5 M. B. Vialtsev, L. O. Tcelykh, A. Y. Bobrovsky and V. V. Utochnikova, *J. Alloys Compd.*, 2022, **924**, 166421.

6 T. V. Balashova, A. P. Pushkarev, A. N. Yablonskiy, B. A. Andreev, I. D. Grishin, R. V. Rumyantcev, G. K. Fukin and M. N. Bochkarev, *J. Lumin.*, 2017, **192**, 208–211.

7 A. Nonat, T. Liu, O. Jeannin, F. Camerel and L. J. Charbonnière, *Chem. – Eur. J.*, 2018, **24**, 3784–3792.

8 L. Aboshyan-Sorgho, M. Cantuel, S. Petoud, A. Hauser and C. Piguet, *Coord. Chem. Rev.*, 2012, **256**, 1644–1663.

9 Y. Li, F. Guo, S. Wei, D. Li, J. Zhang, K. Xu and D. Li, *J. Rare Earths*, 2024, **42**, 278–285.

10 E. Debroye and T. N. Parac-Vogt, *Chem. Soc. Rev.*, 2014, **43**, 8178–8192.

11 I. Mamedov, T. N. Parac-Vogt, N. K. Logothetis and G. Angelovski, *Dalton. Trans.*, 2010, **39**, 5721.

12 A. Nithyakumar and V. Alexander, *Dalton. Trans.*, 2015, **44**, 17800–17809.

13 D. J. Lewis, P. B. Glover, M. C. Solomons and Z. Pikramenou, *J. Am. Chem. Soc.*, 2011, **133**, 1033–1043.

14 K. Binnemans, K. A. Gschneidner Jr, J. C. G. Bünzli and V. K. Pecharsky, *Handbook on the Physics and Chemistry of Rare Earths*, 2005, vol. 225, pp. 107–272, DOI: 10.1016/S0168-1273(04)34006-7.

15 D. Zare, Y. Suffren, H. Nozary, A. Hauser and C. Piguet, *Angew. Chem.*, 2017, **129**, 14804–14809.

16 J. C. G. Bünzli, A. S. Chauvin, C. D. B. Vandevyver, S. Bo and S. Comby, *Ann. N. Y. Acad. Sci.*, 2008, **1130**, 97–105.

17 Z. Yang, C. Sun, Y. Lin, H. Lin, J. Gao and H. Lin, *Cell Reports Phys. Sci.*, 2022, **3**, 100950.

18 C. Szíjjártó, E. Pershagen and K. E. Borbas, *Dalton. Trans.*, 2012, **41**, 7660.

19 M. S. Tremblay and D. Sames, *Chem. Commun.*, 2006, 4116.

20 N. Souri, P. Tian, C. Platas-Iglesias, K.-L. Wong, A. Nonat and L. J. Charbonnière, *J. Am. Chem. Soc.*, 2017, **139**, 1456–1459.

21 A. D. Fedichkina, D. S. Koshelev, A. A. Vashchenko, L. O. Tcelykh, A. S. Goloveshkin, V. E. Gontcharenko, E. V. Latipov, A. V. Medved'ko, S. Z. Vatsadze, A. S. Burlov and V. V. Utochnikova, *J. Lumin.*, 2022, **244**, 118702.

22 L. O. Tcelykh, A. A. Vashchenko, A. V. Medved'Ko, A. E. Marciniak, A. A. Aleksandrov, A. S. Goloveshkin, L. S. Lepnev, E. V. Latipov, A. S. Burlov and V. V. Utochnikova, *J. Mater. Chem. C*, 2022, **10**, 1371–1380.

23 D. S. Koshelev, L. O. Tcelykh, R. E. Mustakimov, A. V. Medved'ko, E. V. Latipov, A. A. Pavlov, A. S. Goloveshkin, V. E. Gontcharenko, K. Y. Vlasova, A. S. Burlov, L. S. Lepnev, S. Z. Vatsadze and V. V. Utochnikova, *J. Lumin.*, 2023, **263**, 120054.

24 A. Kovalenko, L. O. Tcelykh, D. Koshelev, A. A. Vashchenko, D. M. Tsymbarenko, A. S. Goloveshkin, A. Aleksandrov, A. Burlov and V. V. Utochnikova, *Dalton. Trans.*, 2022, **51**, 3833–3838.

25 J. H. Forsberg, R. M. Delaney, Q. Zhao, G. Harakas and R. Chandran, *Inorg. Chem.*, 1995, **34**, 3705–3715.

26 G. Otting, *Annu. Rev. Biophys.*, 2010, **39**, 387–405.

27 C. Piguet and C. F. G. C. Geraldes, *Handb. Phys. Chem. Rare Earths*, 2003, **33**, 353–463.

28 A. G. Martynov, O. V. Zubareva, Y. G. Gorbunova, S. G. Sakharov, S. E. Nefedov, F. M. Dolgushin and A. Y. Tsivadze, *Eur. J. Inorg. Chem.*, 2007, **2007**(30), 4800–4807.

29 E. A. Kuzmina, T. V. Dubinina, A. V. Dzuban, V. I. Krasovskii, O. A. Maloshitskaya and L. G. Tomilova, *Polyhedron*, 2018, **156**, 14–18.

30 A. S. Burlov, A. D. Garnovskii, V. A. Alekseenko, A. E. Mistryukov, V. S. Sergienko, V. G. Zaletov, V. V. Lukov and A. V. Khokhlov, *Koord. Khim.*, 1992, **18**, 859–868.

31 N. I. Chernova, Y. S. Ryabokobylko, V. G. Brudz' and B. M. Bolotin, *Chem. Informationsdienst, Anorg. Phys. Chem.*, 1971, **2**(48), DOI: 10.1002/chin.197148233.

32 K. G. Konya, T. Paul, S. Lin, J. Lusztyk and K. U. Ingold, *J. Am. Chem. Soc.*, 2000, **122**, 7518–7527.

33 L. Mancuso, G. Jürjens, J. Hermane, K. Harmrolfs, S. Eichner, J. Fohrer, W. Collisi, F. Sasse and A. Kirschning, *Org. Lett.*, 2013, **15**, 4442–4445.

34 V. Percec, J. G. Rudick, M. Peterca, M. Wagner, M. Obata, C. M. Mitchell, W.-D. Cho, V. S. K. Balagurusamy and P. A. Heiney, *J. Am. Chem. Soc.*, 2005, **127**, 15257–15264.

35 B. Chakraborty, D. Dutta, S. Mukherjee, S. Das, N. C. Maiti, P. Das and C. Chowdhury, *Eur. J. Med. Chem.*, 2015, **102**, 93–105.

36 A. D. Kovalenko, I. S. Bushmarinov, A. S. Burlov, L. S. Lepnev, E. G. Ilina and V. V. Utochnikova, *Dalton. Trans.*, 2018, **47**, 4524–4533.

37 A. D. Kovalenko, A. A. Pavlov, I. D. Ustinovich, A. S. Kalyakina, A. S. Goloveshkin, Ł. Marciniak, L. S. Lepnev, A. S. Burlov, U. Schepers, S. Bräse and V. V. Utochnikova, *Dalton. Trans.*, 2021, **50**, 3786–3791.